Proc. Natl. Acad. Sci. USA
Vol. 82, pp. 3539–3542, June 1985
Biochemistry

Alternative conformations in *Escherichia coli* 16S ribosomal RNA

(partial denaturation/electron microscopy/RNA structure)

BARBARA K. KLEIN, ARTHUR STADEN, AND DAVID SCHLESSINGER

Division of Biology and Biomedical Sciences, Washington University School of Medicine, Box 8093, St. Louis, MO 63110

Communicated by E. Peter Geiduschek, January 25, 1985

ABSTRACT **Partially denatured 16S rRNA from 30S ribosomes shows features of secondary structure in electron microscopy that correspond to the well accepted secondary structure model derived from chemical modification and phylogenetic data. However, a very different conformation is seen in precursor 16S rRNA sequences contained within 30S pre-rRNA transcripts: the major 5′-terminal loop is absent, and several additional quite stable large loops, symmetrically placed in the molecule, are present. Features of the alternative structure are also seen in mature 16S rRNA from *Escherichia coli* and from two *Bacillus* species when heated in certain buffers. Microscopy thus reveals specific features of alternative conformations and their relative stabilities, suggesting a possible transition during ribosome formation.**

The same unique secondary structure has been inferred for 16S ribosomal RNA both free in solution and in ribosomes based on phylogenetic comparisons combined with studies of the relative resistance of double-stranded regions to nucleases and chemical modification (1, 3–5). Electron microscopy of 16S rRNA and partially denatured 30S ribosomes is also consistent with this secondary structure model (2, 6), which we refer to here as conformation I.

We have therefore been surprised to find loops much larger than any in conformation I in the 16S rRNA sequence within the large ("30S") precursor to rRNA. Similar alternative features can be seen in mature 16S rRNA, both from *Escherichia coli* and from two *Bacillus* species after a heating step. Here we describe initial studies of the relationship between alternative features and conformation I.

MATERIALS AND METHODS

RNA Isolation. The 16S rRNA was isolated from 30S subunits from *E. coli* strain D10, *Bacillus subtilis*, or *Bacillus stearothermophilus* grown in Luria broth. The 30S pre-rRNA was isolated from strain AB301/105 (7–9) cells. In all cases, cells were ground for 1 min at 0°C with twice their weight of alumina. To obtain 16S rRNA, 30S ribosomes were isolated and treated with 0.5% sodium dodecyl sulfate and 100 μg of proteinase K per ml (2, 10) before the 16S rRNA was purified by sucrose gradient centrifugation. For 30S pre-rRNA, the crude extract was directly treated with sodium dodecyl sulfate and proteinase K before the RNA was purified by the same sucrose gradient procedure.

Heating Protocols. Four heating protocols were used. (*i*) The 16S rRNA (70 μg/ml) was heated at 50°C for 30 min in 10 mM NaCl/10 mM Hepes, pH 7.8/5 mM EDTA, and then allowed to cool slowly to room temperature at a rate of ≈10°C per hour. (*ii*) The 16S rRNA was heated for 30 min at 50°C in 200 mM Tris acetate, pH 5.5/10 mM EDTA/1% sodium dodecyl sulfate, and precipitated with 70% ethanol to remove the detergent before preparation for electron microscopy. (*iii*) The 16S rRNA was incubated under RNA·DNA hybridization conditions (55°C for 1 hr in 100 mM Hepes, pH 7.8, containing either 50% or 70% formamide, 400 mM NaCl, and 10 mM EDTA). (*iv*) The 16S rRNA was heated as described for protocol *i*, but it was immediately plunged into ice water.

Electron Microscopy and Data Analysis. The 16S rRNA samples were prepared for electron microscopy (2, 10) using a hyperphase of 50% formamide/10 mM Tris·HCl, pH 8.0/50 mM NaCl, and either 5 mM EDTA or 1 mM Mg^{2+}. The 30S pre-rRNA was spread from a hyperphase of 70% formamide/10 mM Tris·HCl, pH 8.0, containing 50 or 80 mM NaCl and 0.5 mM $MgCl_2$.

To quantitate loop patterns, photographic enlargements of individual molecules were digitized directly into the VAX 11/780 computer for analysis (2). All full-length molecules with traceable contours (>90% of the molecules in each field) were used.

For all conditions examined in this study, the mean molecular length of 16S rRNA was 0.48–0.52 μm, with a standard deviation of 0.07 μm, as expected (2).

A consensus structure of loops in a group of molecules was inferred with the techniques used earlier for unheated 16S rRNA of *E. coli* (2) and *B. stearothermophilus* (11). Briefly, the length of each loop and the distance of its midpoint from the ends of a molecule were first determined. Loops <500 nucleotides (nt) were considered first, because they include all the features found in conformation I and unheated rRNA. Absolute orientations had already been determined for these loops (2); they fall in one of three "domains," each about one-third of the molecule (as in Fig. 3*A* below). The most frequent features are a 5′-terminal loop and two 3′-subterminal loops; these were used to orient molecules and locate the midpoint of each loop in other data sets. The numbers and sizes of composite loops were then determined by fitting the loop size distribution within each domain with a set of gaussian peaks to estimate significance and standard deviations. (In general, the standard deviations of loop sizes range from 30 to 70 nt, and those of midpoint locations vary from 50 to 130 nt.)

For heated rRNA and pre-rRNA, a histogram of loop frequency versus size revealed four size classes of loops (see Fig. 2*B*), separated by minima: loops <500 nt, 500–800 nt, 800–1100 nt, and >1100 nt. The loops in each class were again located by comparison to smaller loops. Their placement was also facilitated because they tended to be symmetrical within the rRNA (see Fig. 2 *B* and *H*). The consensus loops were checked by a second gaussian fitting procedure on each size class of large loops.

Thermodynamic Calculations and Primary Sequence Analysis. The relative free energy of base-paired regions was estimated as described (10–13). Possible base-paired interactions were generated by a program of W. Barnes and M. Zyda (personal communication) searching for matches of 7/8 or 8/8 base pairs (not including G·U pairs). Base-paired regions with end points similar to those expected from

The publication costs of this article were defrayed in part by page charge payment. This article must therefore be hereby marked "*advertisement*" in accordance with 18 U.S.C. §1734 solely to indicate this fact.

Abbreviation: nt, nucleotide(s).

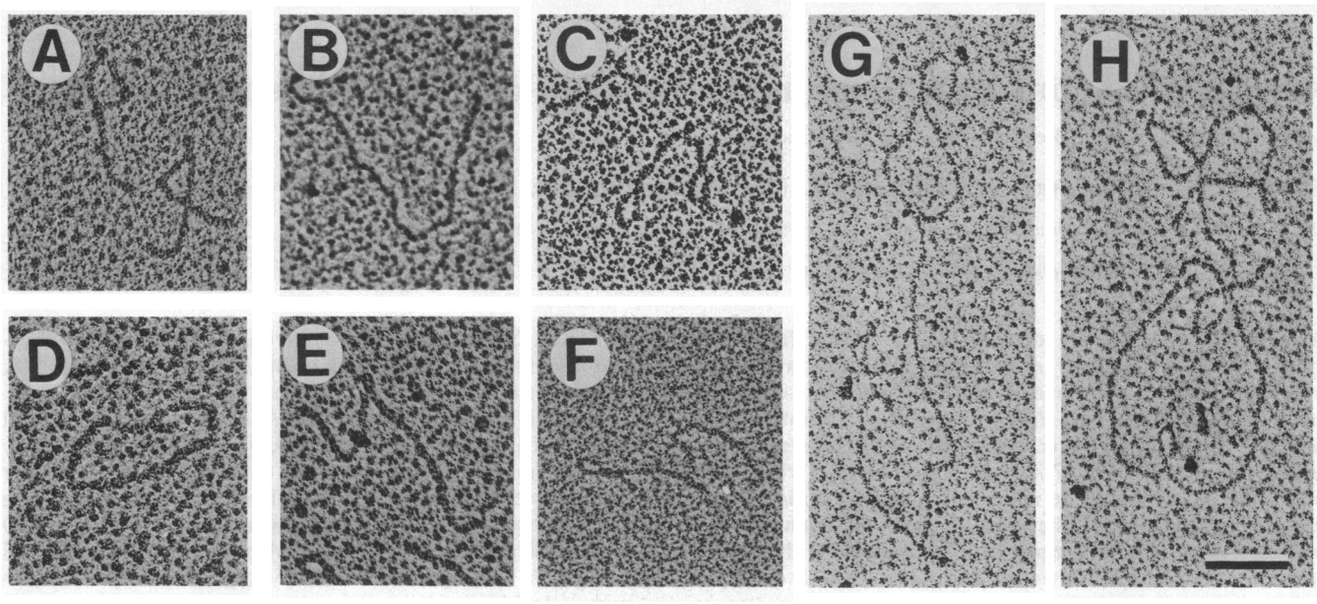

FIG. 1. rRNA molecules spread before and after heating. (*A*) *E. coli* 16S rRNA heated by protocol 1 and prepared for microscopy in 50 mM NaCl/5 mM EDTA. (*B*) Unheated 16S rRNA in 50 mM NaCl/5 mM EDTA. (*C*) Unheated 16S rRNA in 50 mM NaCl/1 mM $MgCl_2$. (*D*) *B. stearothermophilus* 16S rRNA treated as in *A*. (*E*) *E. coli* 16S rRNA heated and quickly cooled (protocol 4) and spread as in *A*. (*F*) As in *E*, but spread in 50 mM NaCl/1 mM $MgCl_2$. (*G* and *H*) Two molecules of 30S pre-rRNA spread as described in *Materials and Methods*, showing long-range and short-range loops. (Bar = 0.1 μm.) (×93,795.)

electron microscopy results were checked using the Zuker 1 energy minimization program (12, 13) with short segments in the regions predicted by the dot matrix results. Possible interactions A, B, and C (see below) were defined in this way.

RESULTS

Previous experiments with 16S rRNA identified a discrete set of loops that fell within three location domains. The prominent loops included one at the 5′ end and several near the 3′ end (Fig. 1*C*; see also Fig. 3 and ref. 2). In all, nine major loops, all <500 nt long, were identified from the analysis of a large number of individual molecules; their sizes and positions are listed in Table 1 (columns 5 and 6). These loops, characteristic of conformation I, were seen at high frequencies only in the presence of either ribosomal proteins or >0.5 mM Mg^{2+}. For example, 86 molecules of RNA spread in 50 mM NaCl and 1 mM Mg^{2+} had an average of 2.6 ± 0.7 loops per molecule (as in Fig. 1 *C* and *F*). In contrast, 118 molecules also spread in 50 mM NaCl but with 5 mM EDTA instead of Mg^{2+} ions showed only 0.8 ± 0.8 loops per molecule (Fig. 1 *B* and *E*).

Very different results were seen for the precursor 16S rRNA loop in the large primary rRNA transcript of *E. coli* (the "30S pre-rRNA"; refs. 7–9). Examples are shown in Fig. 1 *G* and *H* from among 204 molecules and a number of preparations, all of which included Mg^{2+} ions in the spreading buffers. A detailed analysis of large numbers of pre-rRNA molecules will be presented elsewhere; but Table 1 (columns 1 and 2) lists a set of consensus loops that can be compared with those in conformation I (columns 5 and 6). In addition to five smaller loops, which are listed on the same lines as their probable conformation I counterparts, three larger loops were seen.

The large loops, unlike the smaller ones, were quite stable even in the absence of Mg^{2+} ions. Since they were so stable in pre-rRNA, we asked whether they could be part of a more stable structure that might form when conformation I was denatured in mature 16S rRNA. After heating by any of protocols *i* to *iii*, we found that mature rRNA also showed alternative conformational features.

Large terminal or central loops were seen (Fig. 1*A*), and the number of loops per molecule increased, even in rRNA spread in the absence of Mg^{2+} ions, from 0.8 in unheated rRNA to 2.0 in 269 heated molecules. The increase in the average number of loops per molecule and especially in large loops is clear in Fig. 2 (compare *A* and *B* to *C* and *D*) (the panels at the left are rotated 90° to yield the panels at the right, in order to make the larger loops clearer).

Molecules spread in Mg^{2+} showed the same large loops and more small loops, and they were therefore often difficult to trace; thus, we have further analyzed loops only in molecules

Table 1. Loop sizes and locations in 16S rRNA

	Precursor		Heated		Unheated	
Domain	Size	Midpoint	Size	Midpoint	Size	Midpoint
			Loops <500 nt long			
I	140	350	210	230	110	300
	—	—	440	280	370	220
II	100	760	150	720	110	710
	220	730	230	720	190	740
	—	—	300	760	280	700
III	160	1290	180	1060	150	1170*
	—	—	—	—	240	1170
	310	1220	260	1160	260	1170
	—	—	410	1150	460	1170
			Loops >500 nt long†			
	—	—	550	1180		
	610	730	720	810		
	—	—	950	880		
	1000	570	1000	510		
	1240	740	1360	810		

The length and location of the midpoint of each consensus loop are shown for the 16S rRNA sequence within 30S pre-rRNA; for rRNA heated by protocols 1, 2 or 3; and for unheated 16S rRNA (2). Loops that may correspond in different samples are on the same line. See *Materials and Methods* for error estimates.

*The four loops in domain III are only approximate (2).

†The three loops in pre-rRNA may be determined by interactions A, B, and C, respectively (see text).

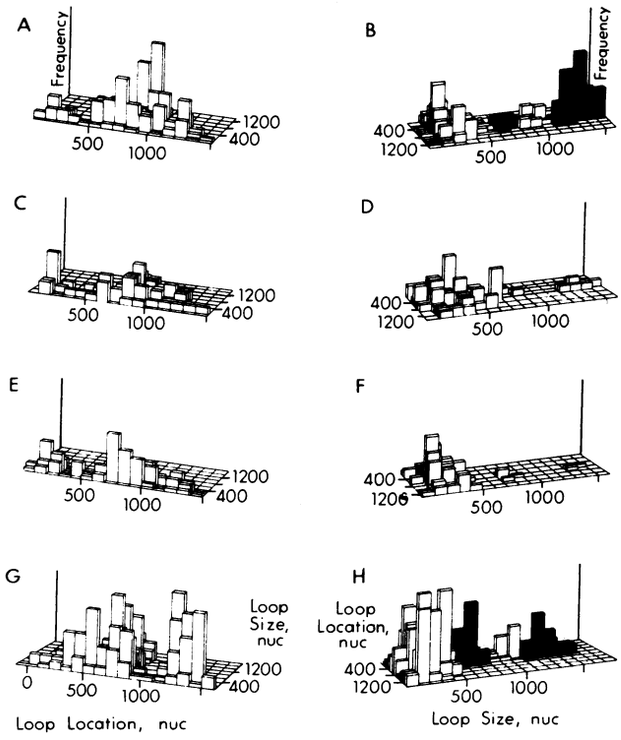

FIG. 2. Frequency, location, and size of loops in rRNA. The left panels are rotated 90° to yield the right panels. (*A* and *B*) rRNA heated (protocol 1). (*C* and *D*) Unheated RNA spread for microscopy in 50% formamide/50 mM NaCl/5 mM EDTA. (*E* and *F*) Heated and quickly cooled RNA (protocol 4) and spread as in *C* and *D*. (*G* and *H*) Loops in the 16S sequence within 30S pre-rRNA. (*B* and *H*) Loops grouped into size classes, alternately white and black, <500, 500–800, 800–1100, and >1100 nucleotides (nuc); the three largest size groups could include putative interactions A–C, respectively.

spread without Mg^{2+}. From the analysis of >100 molecules, the structure includes small loops similar to those in unheated rRNA (Fig. 3 *A* and *B*; Table 1, compare columns 3 and 4 to 5 and 6), but it is dominated by loops much larger than the largest loop of 460 nt in unheated 16S rRNA. These are grouped into size classes (alternately black and white in Fig. 2 *B* and *H*). Five inferred large loops are listed in Table 1; three of them may correspond to the large loops in pre-rRNA.

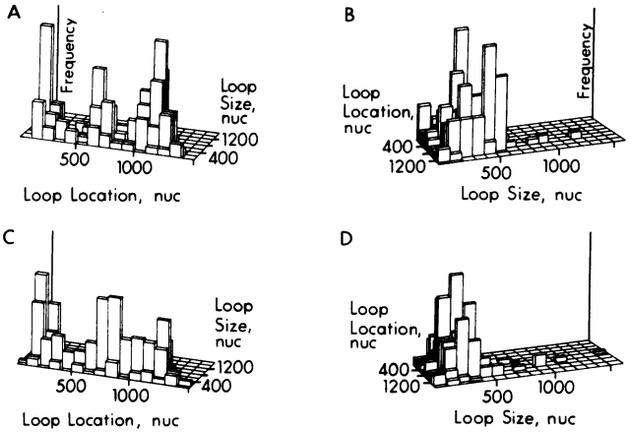

FIG. 3. Frequency, location, and size of loops in 16S rRNA in 1 mM Mg^{2+} without heating and after heating and rapid cooling (protocol 4). Left panels are rotated 90° to give right panels. (*A* and *B*) Unheated rRNA as in Fig. 1*C*. (*C* and *D*) rRNA heated and quickly cooled in EDTA and then spread for microscopy as in Fig. 1*F*. nuc, Nucleotides.

Such observations were extended to 16S rRNA samples from two disparate species: *B. subtilis* and *B. stearothermophilus*. The rRNA from both these species showed a structure similar to that in *E. coli* (cf. ref. 11), and after heating, each gave rise to a population of molecules with very large loops (e.g., Fig. 1*D*). In all cases, heated samples of *E. coli* and *Bacillus* 16S rRNA showed >50% of the molecules with superficially similar symmetrical loops >700 nt long.

To determine whether this transition to an alternative conformation could be reversed, "renaturation" experiments were performed. When molecules were heated in low salt buffer and then quickly cooled (protocol *iv*), conformation I was at least partially restored and many of the large loops were lost. Results were the same whether quick cooling was done immediately after an initial heating, or after a sample had been heated and slow-cooled (as in protocol *i*) and then reheated. For example, after heating in 10 mM NaCl without Mg^{2+} (Fig. 2 *E* and *F*), the number of loops per molecule seen in 111 molecules at 50 mM NaCl and 5 mM EDTA dropped from 2.0 to ≈1.2. This can be compared to the value of 0.8 in unheated rRNA in the same buffer (Fig. 2 *C* and *D*). The extra loop that still remains is seen in Fig. 2 *E* and *F* as a small hairpin (150 nt) near the center of the molecule; it seems to be distinct from the loops found in this region in unheated rRNA (Table 1).

Fig. 3 shows the result of heating in EDTA (by protocol *iv*, which promotes renaturation) and subsequent preparation for electron microscopy in buffer containing 1 mM Mg^{2+}. The number of loops per molecule in 208 molecules was thereby increased to the same value (2.4 ± 0.9) found in an unheated 16S rRNA preparation spread in the presence of Mg^{2+} ions (cf. Fig. 3). Furthermore, the loops in domain I were now the same ones seen in conformation I (110 and 370 nt long, with midpoints at nt 300 and 220, respectively). The other two domains showed less complete restoration of conformation I. Domain II again showed a dominant 150-nt hairpin; and both samples (Figs. 2*E* and 3*C*) had loops centered at 800–1100 nt, a region of little structure in the unheated rRNA.

DISCUSSION

In vitro, the conversion of heated rRNA from one form to another may be analogous to transitions in several heated tRNAs and 5S RNA (14). Energy is required to disrupt stacking interactions that stabilize each conformation. One possibility is that when molecules are heated, interactions of conformation I melt, and the stronger long-range interactions of the alternative conformation form and are retained during slow cooling (Fig. 2 *A* and *B*). Rapid cooling would rather facilitate the formation of the shorter-range interactions of conformation I (although the transition may not be complete; compare Fig. 2 *E* and *F* to *C* and *D* and Fig. 3 *C* and *D* to *A* and *B*).

The alternative features reported here may exist in *E. coli* cells, at least in pre-rRNA, for two reasons. First, they are seen in pre-rRNA extracted mildly by a number of procedures—including the same conditions in which only ≈1% of extracted 16S rRNA shows similar features. They are seen in a variety of buffers, both in the presence of Mg^{2+} ions, which stabilize rRNA structure (1–5, 10, 11), and in their absence. Furthermore, high temperature or other denaturing conditions have been required to convert one conformation to another (see Figs. 1–3 and below). One would, therefore, not expect to shift one form to another during mild extraction. Second, others have isolated some double-stranded fragments from 16S rRNA containing the interactions that may define some of the large loops (see refs. 4, 15, and 16, and see below).

We have tried to define better the molecular interactions underlying the large loops of Table 1. The stabilities of the

loops in partially denatured 16S rRNA (2, 11) generally correlate with the ΔG° values of their short base-paired stems (1); and since the large alternative loops are more stable in denaturing conditions, we searched for stronger possible stems than those in conformation I. We found three possible interactions in the vicinity of observed loops (±120 nt at each terminus). Interaction A is a loop of 667 nt pairing bases 386–400 with 1053–1068, centered at 727 nt along the contour of 16S rRNA ($\Delta G^{\circ} = -36.6$ kcal; 1 cal = 4.184 J); interaction B has a loop size of 1089 nt, pairing bases 34–44 with 1123–1133, with a midpoint location of 584 nt ($\Delta G^{\circ} = -26.7$ kcal); and interaction C is a set of three colinear base-paired regions, pairing bases 87–146 with 1378–1435, with loop sizes ranging from 1250 to 1350 nt centered at ≈770 nt; the most stable segment has a relative free energy of −28.5 kcal. The loops that correspond most closely to interactions A, B, and C are indicated in Table 1 and are found within the corresponding size classes of loops in Fig. 2 *B* and *H*.

The tentatively assigned interactions A–C would disrupt features of conformation I and define alternative forms. A and B would eliminate both 5′-terminal loops as well as a weakly base-paired region at the tip of the hairpin in the 3′ domain (see figure 4 in ref. 1). Interaction C would partially disrupt part of a small hairpin in the 5′ region, as well as the largest most stable loop in the 3′ domain. Preliminary analyses of single molecules indicate that molecules containing the largest loops indeed contain very few 5′-terminal loops.

If interactions A–C were involved in ribosome formation or rRNA processing, one would expect strong evolutionary conservation in eubacteria [but not in eukaryotes, since they show no double-stranded stems at the base of rRNA sequences in pre-rRNA and have a very different mechanism of processing (17)]. Available sequence data indeed show strong conservation between the evolutionarily distant prokaryotes *E. coli* and *B. stearothermophilus* (1). For example, the sequences putatively involved in interaction A are essentially identical in the two species. A universal role for such interactions in translation has also been considered, since interactions A and B are at least partially conserved in species as evolutionarily advanced as *Xenopus laevis* (5, 15, 18). But of course the speculations that an alternative conformation may be conserved and may be an intermediate in ribosome formation or function require much more rigorous testing.

In vivo, factors other than high temperature must promote one or another conformation. In 30S pre-rRNA, the stem at the base of 16S rRNA (9) may promote and stabilize alternative conformational features by bringing appropriate regions of the RNA into proximity. The transition of the 16S rRNA to conformation I might also be facilitated by r proteins, which stabilize interactions of conformation I (2). Such a shift in structure might be related to the large conformational change that has been detected during 30S ribosome assembly (19). Also, pre-rRNAs seem to function more efficiently than 16S rRNA in 30S particle formation (20, 21), and alternative conformational features may favor a critical step.

We acknowledge gratefully the permission of M. Zuker to use the RNA folding program he developed at the National Research Council of Canada; it was implemented for us on the VAX 11/780 by Monty Brandenberg. These studies have been supported by Grant PCM-8017402 from the National Science Foundation, National Institutes of Health Grant GM 10447, National Institutes of Health Postdoctoral Fellowship 5-F32-GM 08012 to B.K.K., and auxiliary support from the Monsanto Biomedical Research Agreement.

1. Woese, C. F., Gutell, R., Gupta, R. & Noller, H. F. (1983) *Microbiol. Rev.* **47**, 621–699.
2. Klein, B. K., Forman, P., Shiomi, Y. & Schlessinger, D. (1984) *Biochemistry* **23**, 3927–3933.
3. Brimacombe, R., Maly, P. & Zwieb, C. (1983) *Prog. Nucleic Acid Res. Mol. Biol.* **28**, 48.
4. Glotz, C. & Brimacombe, R. (1980) *Nucleic Acids Res.* **8**, 2377–2395.
5. Stiegler, P., Carbon, P., Zuker, M., Ebel, J. P. & Ehresmann, C. (1981) *Nucleic Acids Res.* **9**, 2153–2172.
6. Spirin, A. S., Serdyuk, I. N., Shpungin, J. L. & Vasiliev, V. D. (1979) *Proc. Natl. Acad. Sci. USA* **76**, 4867–4871.
7. Dunn, J. J. & Studier, F. W. (1973) *Proc. Natl. Acad. Sci. USA* **70**, 3296–3300.
8. Nikolaev, N., Silengo, L. & Schlessinger, D. (1973) *Proc. Natl. Acad. Sci. USA* **75**, 3593–3598.
9. Young, R. A. & Steitz, J. A. (1978) *Proc. Natl. Acad. Sci. USA* **75**, 3593–3598.
10. Klein, B. K., King, T. C. & Schlessinger, D. (1983) *J. Mol. Biol.* **168**, 809–830.
11. Klein, B. K., Romero, J. & Schlessinger, D. (1985) *J. Bacteriol.*, in press.
12. Cech, T. R., Tanner, N. K., Tinoco, I., Jr., Weir, B. R., Zuker, M. & Perlman, P. S. (1983) *Proc. Natl. Acad. Sci. USA* **80**, 3903–3907.
13. Jacobson, A. B., Good, L., Simonetti, J. & Zuker, M. (1984) *Nucleic Acids Res.* **12**, 45–52.
14. Crothers, D. M. & Cole, P. E. (1978) in *Transfer RNA*, ed. Altman, S. (MIT Press, Cambridge, MA), pp. 196–247.
15. Noller, H. F. (1980) in *Ribosomes*, eds. Chambliss, G., Craven, G. R., Davies, J., Davis, K., Kahan, L. & Nomura, M. (University Park Press, Baltimore), pp. 1–22.
16. Zwieb, C., Glotz, C. & Brimacombe, R. (1981) *Nucleic Acids Res.* **9**, 3621–3640.
17. Goldman, W. E., Goldberg, G., Bowman, L. H., Steinmetz, D. & Schlessinger, D. (1983) *Mol. Cell. Biol.* **3**, 1488–1500.
18. Carbon, P., Ebel, J. P. & Ehresmann, C. (1981) *Nucleic Acids Res.* **9**, 2325–2333.
19. Nomura, M. & Held, W. A. (1974) in *Ribosomes*, eds. Nomura, M., Tissieres, A. & Lengyel, P. (Cold Spring Harbor Laboratory, Cold Spring Harbor, NY), pp. 193–223.
20. Mangiarotti, G., Turco, E., Perlo, C. & Altruda, F. (1975) *Nature (London)* **253**, 569–571.
21. Nikolaev, N. & Schlessinger, D. (1974) *Biochemistry* **13**, 4272–4278.